Proc. Natl. Acad. Sci. USA
Vol. 96, pp. 6199–6204, May 1999
Cell Biology

PTEN modulates cell cycle progression and cell survival by regulating phosphatidylinositol 3,4,5,-trisphosphate and Akt/protein kinase B signaling pathway

HONG SUN*†, RALF LESCHE‡§, DA-MING LI*§, JOANNA LILIENTAL‡¶, HUI ZHANG*, JING GAO‡, NADIA GAVRILOVA*, BRENDA MUELLER‖, XIN LIU‖, AND HONG WU†‡

*Department of Genetics, Yale University School of Medicine, 333 Cedar Street, New Haven, CT 06520; and ‡Howard Hughes Medical Institute and Department of Molecular and Medical Pharmacology, and Departments of ¶Microbiology and Molecular Immunology, and ‖Pathology and Laboratory Medicine, University of California, 650 Circle Drive South, Los Angeles, CA 90095-1735

Communicated by Harvey F. Lodish, Massachusetts Institute of Technology, Cambridge, MA, March 29, 1999 (received for review October 26, 1998)

ABSTRACT **To investigate the molecular basis of PTEN-mediated tumor suppression, we introduced a null mutation into the mouse *Pten* gene by homologous recombination in embryonic stem (ES) cells. *Pten*$^{-/-}$ ES cells exhibited an increased growth rate and proliferated even in the absence of serum. ES cells lacking PTEN function also displayed advanced entry into S phase. This accelerated G_1/S transition was accompanied by down-regulation of p27^{KIP1}, a major inhibitor for G_1 cyclin-dependent kinases. Inactivation of PTEN in ES cells and in embryonic fibroblasts resulted in elevated levels of phosphatidylinositol 3,4,5,-trisphosphate, a product of phosphatidylinositol 3 kinase. Consequently, PTEN deficiency led to dosage-dependent increases in phosphorylation and activation of Akt/protein kinase B, a well-characterized target of the phosphatidylinositol 3 kinase signaling pathway. Akt activation increased Bad phosphorylation and promoted *Pten*$^{-/-}$ cell survival. Our studies suggest that PTEN regulates the phosphatidylinositol 3,4,5,-trisphosphate and Akt signaling pathway and consequently modulates two critical cellular processes: cell cycle progression and cell survival.**

The tumor susceptibility gene encoding PTEN/MMAC1/TEP1 (1–3) is mutated at high frequency in many primary human cancers and several familial cancer predisposition disorders (4). PTEN contains the sequence motif that is highly conserved in the members of the protein tyrosine phosphatase family. PTEN has been shown *in vitro* to possess phosphatase activity on phosphotyrosyl, phosphothreonyl-containing substrates (3, 5) and more recently, on phosphatidylinositol 3,4,5-trisphosphate (PIP3), a product of phosphatidylinositol 3 (PI3) kinase (6). Many cancer-related mutations have been mapped within the conserved catalytic domain of PTEN, suggesting that the phosphatase activity of PTEN is required for tumor suppressor function. In addition, wild-type PTEN, but not mutant derivatives lacking phosphatase activity, suppresses the growth of glioblastoma cells and their tumorigenecity in nude mice (7–9), confirming the functional relevance of the PTEN phosphatase domain for tumor suppression. Very recently, inactivation of PTEN in a mouse model has confirmed the role of PTEN as a bona fide tumor suppressor (10). However, the exact function of PTEN in regulation of cell growth and tumorigenesis remains unclear.

In this study, we have investigated the molecular basis underlying the tumor suppression function of PTEN by using a combination of molecular genetic, cell biological, and biochemical approaches. We have identified PIP3, a product of PI3 kinase, as an intracellular target of PTEN. Our studies suggest that PTEN acts as a negative regulator for the PI3-kinase/Akt signaling pathway, which controls and coordinates two major cellular processes: cell cycle progression and cell death.

The publication costs of this article were defrayed in part by page charge payment. This article must therefore be hereby marked "*advertisement*" in accordance with 18 U.S.C. §1734 solely to indicate this fact.

PNAS is available online at www.pnas.org.

MATERIALS AND METHODS

Generation of *Pten*$^{-/-}$ Embryonic Stem (ES) and Mouse Embryonic Fibroblasts (MEF) Cell Lines. Genomic DNA clones corresponding to the *Pten* locus were isolated from an isogenic 129(J1) genomic library (11). The targeting vector, pKO-1, contains the PGKneopA cassette flanked by 8.0-kb *Kpn*I–*Apa*I fragment (5′ arm) and 3-kb *Bam*HI–*Xba*I fragment (3′ arm) in the backbone of pBluescript vector. Linearized pKO-1 plasmid (25 μg) was electroporated into 1×10^7 J1 ES cells as described (11). G418^r ES clones were isolated and expanded. Genomic DNAs were prepared for Southern blot analysis. To obtain ES clones homozygous for the *Pten* deletion, heterozygous ES clones were subjected to a higher G418 selection (5 mg/ml). Homozygous deletion was confirmed by Southern blot analysis. ES cell clones homozygous for the *Pten* deletion were injected into BALB/c blastocysts. Chimeric embryos were collected at embryonic day 14–15 gestation. MEF cells were prepared and subjected to G418 (400 μg/ml) selection for 10 days to eliminate wild-type (WT) cells. *Pten* deletion then was further confirmed by Southern and Western blot analyses.

Colcemid Block and Mitotic Shake-Off. ES cells were passaged twice without feeder support to remove *Pten*$^{+/+}$ feeder cells. Mitotic cells were prepared according to Savatier *et al.* (12). An equal number of mitotic cells were seeded on gelatinized plates and incubated to allow synchronized cell cycle reentry. Cytospin of collected cells followed by Wright staining showed that this procedure yielded 90–95% mitotic cells (data not shown).

Antibodies, Western Blot Analysis, and Kinase Assay. Cell lysate preparation, immunoprecipitation, Western blot analysis, and histone H1 kinase assay were carried out as described (9). Antibodies specific for p27^{KIP1} (sc-528), cyclin D1 (R-124), p21$^{CIP1/WAF1}$ (sc-397), and mouse cyclin E (sc-481) were obtained from Santa Cruz Biotechnology. Antibodies specific for cyclin A, cyclin-dependent kinase (CDK2) (13), and PTEN (9) have been described. Antibodies for Bad (B36420) and focal adhesion kinase (FAK) (F15020) were from Transduction Laboratories, Lexington, KY. Antiphosphotyrosine antibody 4G10 and anti-

Abbreviations: ES, embryonic stem; PIP, phosphatidylinositol 4-phosphate; PI3, phosphatidylinositol 3; PIP2, phosphatidylinositol 4,5-bisphosphate; PIP3, phosphatidylinositol 3,4,5,-trisphosphate; MEF, mouse embryonic fibroblasts; WT, wild type; CDK, cyclin-dependent kinase; PKB, protein kinase B; MAPK, mitogen-activated protein kinase; IGF-I, insulin-like growth factor I; TUNEL, terminal deoxynucleotidyltransferase-mediated UTP end labeling; FAK, focal adhesion kinase.

†To whom reprint requests should be addressed. e-mail: hong.sun@yale.edu or hwu@mednet.ucla.edu.
§R.L. and D.-M.L. contributed equally to this work.

p85 subunit of PI3 kinase antibody (06–195) were obtained from Upstate Biotechnology. Anti-Akt/protein kinase B (PKB) and anti-mitogen-activated protein kinase (MAPK) antibodies were from New England Biolabs.

Phospholipids Analysis. Phospholipid extraction and TLC analysis were performed according to Trynor-Kaplan *et al.* (14). To prepare ^{32}P-labeled molecular weight markers for phosphatidylinositol 3-phosphate, phosphatidylinositol 3,4-bisphosphate, and PIP3, PI3 kinase was immunoprecipitated from insulin-like growth factor (IGF-I)-stimulated 293 cells with anti-p85 antibody and used to phosphorylate the lipid substrates phosphatidylinositol (Sigma), phosphatidylinositol 4-phosphate (PIP) (Boehringer Mannheim), or phosphatidylinositol 4,5-bisphosphate (PIP2) (Boehringer Mannheim) in a reaction containing [^{32}P]-γ-ATP as described (15). The *in vitro* ^{32}P-labeled phosphoinositides, PIP2, and PIP3 then were used as standards for TLC analyses.

Terminal Deoxynucleotidyltransferase-Mediated UTP End Labeling (TUNEL) Assay. Log-phase growing MEF cells were seeded at a density of 5×10^4 cells per 12-mm round coverslip (Fisher Scientific). After attachment, cells were cultured in medium without serum for 72 hr. Cells were fixed in 3.7% formaldehyde/PBS, permeabilized in 0.2% Triton X-100/PBS and stained with rhodamine-phalloidin (Molecular Probes) in 10% normal goat serum/PBS, followed by counterstaining with TUNEL reaction mixture (Boehringer Mannheim). Cells were visualized by using fluorescence microscopy.

RESULTS

Generation of *Pten*$^{-/-}$ ES Cells and Characterization of Their Growth Properties. We introduced a null mutation into the mouse *Pten* gene by homologous recombination in ES cells. Fig. 1*A* shows the targeting vector, pKO-1, in which both transcriptional and translational initiation sites and exons 1–3 of the *Pten* gene were deleted. By using an external probe, an 8.5-kb band corresponding to the targeted allele (Fig. 1*B*, lane 2) was detected in six of 200 G418^r colonies. To facilitate the study of PTEN function at the cellular level, we generated *Pten*$^{-/-}$ ES cells by selecting with a higher dose of G418 (Fig. 1*B*, lane 3). In each of the following experiments, results were repeated and confirmed by using several independent ES clones to avoid potential clonal variations.

In the process of culturing *Pten*$^{+/+}$, *Pten*$^{+/-}$, and *Pten*$^{-/-}$ ES cells, we noticed that the *Pten*$^{-/-}$ ES cells appeared to reach high cell density faster. To determine whether *Pten*$^{-/-}$ cells had altered growth properties, we performed a growth competition experiment. Equal numbers of *Pten*$^{+/+}$ cells were mixed with *Pten*$^{+/-}$ or *Pten*$^{-/-}$ cells and cocultured. Cells were passed every 3 days to avoid growth saturation. During each passage, a fraction of the cell mix was harvested, and genomic DNA was prepared for Southern blot analysis to determine the representation of each cell type. As shown in Fig. 1*B* and quantified in Fig. 1*C*, the intensity of the 8.5-kb band, representing the *Pten* deletion allele (KO), increased significantly from passage 1 to passage 3 (Fig. 1*B*, lanes 5, 7, and 9) while the 23-kb fragment of the WT allele decreased correspondingly, indicating that the percentage of *Pten*$^{-/-}$ cells increased with each passage. At the end of the third passage (corresponding to 13–14 doublings of normal ES cells), the *Pten*$^{-/-}$ ES cells had outgrown the *Pten*$^{+/+}$ cells, as revealed by a dramatic reduction of the WT DNA band (Fig. 1*B*, lane 9) from the final cell population. As a control, when *Pten*$^{+/+}$ and *Pten*$^{+/-}$ cells were cocultured, the ratios between the KO and the WT alleles were largely unaltered during the consecutive passages (Fig. 1*B,* lanes 4, 6, and 8). Because under normal growth conditions, cell death is rare ($< 1\%$), these results suggest that deletion of the *Pten* gene provides cells with a growth advantage, possibly by shortening the cell cycle time (see below).

Pten$^{+/+}$, *Pten*$^{+/-}$, and *Pten*$^{-/-}$ ES cells were compared for serum dependency. ES cells were cultured in parallel for 4 days in media containing reduced concentrations of serum. As shown in Fig. 1*D*, even in the medium without serum, *Pten*$^{-/-}$ ES cells were able to proliferate, and the total cell number was increased. In addition, *Pten*$^{-/-}$ ES cells survived better in reduced serum conditions. In serum-free medium, most of the *Pten*$^{+/+}$ and *Pten*$^{+/-}$ ES cells lost their viability in 2–3 days and detached from feeder layers (Fig. 1*E*, *a* and *b*). However, approximately 80% of *Pten*$^{-/-}$ ES cells remained and proliferated to form small colonies (Fig. 1*E*, *c* and *d*). Thus, the sustained growth of *Pten*$^{-/-}$ cells in the absence of serum could reflect a combination of increased cell survival and enhanced cell proliferation of *Pten*$^{-/-}$ ES cells.

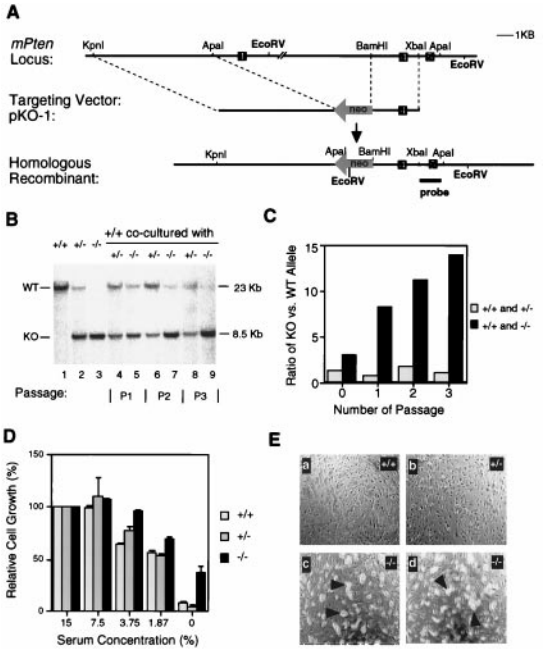

FIG. 1. Inactivation of the mouse *Pten* gene and the growth properties of *Pten*$^{-/-}$ ES cells. (*A*) A restriction map of the genomic region containing the *Pten* gene is shown at the top, with exons depicted. The targeting vector pKO-1 is shown in the middle. A restriction map of the predicted recombinant harboring the deleted allele is shown at the bottom. (*B*) Southern blot analysis. Lanes 1–3: DNA from *Pten*$^{+/+}$ (+/+, lane 1), heterozygous (+/−, lane 2), and homozygous (−/−, lane 3) ES cell cultures. Lanes 4–9: DNA from cocultured ES cells. An equal number (4×10^5) of +/+ cells were cocultured with +/− cells in 33-mm dish (lanes 4, 6, and 8). Alternatively, an equal number of +/+ cells were cocultured with −/− cells (lanes 5, 7, and 9). DNA isolated from the indicated cultures were analyzed after one, two, or three passages. After *Eco*RV digestion, 23-kb and 8.5-kb bands, corresponding to the WT allele or the targeted allele (KO), respectively, could be detected by using an external probe. (*C*) Quantification of the amount of radioactivity in the hybridized restriction fragment corresponding to the WT allele (23 kb) or the *Pten* deletion allele (KO, 8.5 kb). The relative hybridization intensity of KO versus WT band in cocultures is presented. (*D*) ES cells (1×10^5 cells/well in 24-well plate) were grown in media containing the indicated serum concentrations. Four days later, cells were counted. The relative cell growth was calculated by using cell numbers in 15% serum condition as 100%. Each value represents the average (±SD) obtained from a duplicate set of experiments. (*E*) WT (+/+, *a*), heterozygous (+/−, *b*) and two independent homozygous (−/−, *c* and *d*) ES cell lines were grown in serum-free medium for 4 days. Although no ES colonies, except the background feeder cell layers, were seen in the WT and heterozygous ES cultures (*a* and b, respectively), visible ES cell colonies (indicated by the arrowheads) were present in homozygous ES cultures (*c* and *d*). Scale bar: 200 μM.

Advanced G_1 Cell Cycle Progression in *Pten*$^{-/-}$ Cells Correlates With Down-Regulation of p27^{KIP1}. The ability of *Pten*$^{-/-}$ cells to proliferate under reduced serum conditions and their higher growth rate raised the possibility that deletion of the *Pten* gene may affect cell cycle progression. Our recent studies indicated that transient expression of the *PTEN* gene in a human glioblastoma cell line caused G_1 cell cycle arrest, suggesting that

PTEN may play a role in the G_1/S transition (9). These observations prompted us to examine whether *Pten*$^{-/-}$ cells have an accelerated cell cycle progression from G_1 into S phase.

ES cells are rapidly proliferating cells. Under normal growth conditions, we observed that about 60–70% of ES cells were in S phase. Because ES cells do not exhibit contact inhibition and respond poorly to serum deprivation, we used the mitotic shake-off method (12) for synchronization. Mitotic cells were collected after colcemid treatment and then released into fresh medium. S-phase entry was monitored by incorporation of [^{3}H]thymidine. Consistent with a previous report (12), [^{3}H]thymidine incorporation occurred about 3 hr after release from the mitotic block (Fig. 2*A*), suggesting that ES cells have a G_1 phase of about 2–3 hr. *Pten*$^{-/-}$ cells reproducibly showed an earlier (approximately 0.5–1 hr advance) and more synchronized entry into S phase compared with *Pten*$^{+/+}$ cells. Because the synchronized ES cells have a cell cycle time of approximately 9–10 hr, the advanced S-phase entry we observed in *Pten*$^{-/-}$ cells shortened the cell cycle time by 5–10%, which could have a significant impact on the growth rate of *Pten*$^{-/-}$ cells.

To determine the cause of early S-phase entry in PTEN-deficient cells, we examined the levels of G_1 cell cycle regulators, including two major G_1 CDK inhibitors, p21$^{CIP1/WAF1}$ and p27^{KIP1}. p21$^{CIP1/WAF1}$ and p27^{KIP1} are involved in G_1/S progression, and their levels are known to be regulated by extracellular stimuli (16). Consistent with previous reports (17), p21 was not detectable in ES cells (data not shown), suggesting that p21 is not the major G_1 CDK inhibitor in ES cells. However, p27 was readily detectable in ES cells and its levels were oscillated in the cell cycle (Fig. 2*B*). In *Pten*$^{+/+}$ cells, p27 levels were low during mitosis (0 hr), transiently increased as cells entered the G_1 phase (2–3 hr), modestly reduced at the 4-hr time point, and returned to the basal level after 6 hr. In *Pten*$^{-/-}$ cells, however, both basal (0 hr) and induced levels of p27 during G_1 phase (2 and 3 hr) were significantly reduced. In addition, down-regulation of p27 occurred more rapidly in *Pten*$^{-/-}$ cells. By 4 hr, nearly 75% reduction in the p27 level was observed. As a control, the levels of cyclin D1, a major G_1 cyclin, were comparable in both *Pten*$^{+/+}$ and *Pten*$^{-/-}$ cells and were relatively constant throughout the cell cycle (Fig. 2*B*).

The binding of p27 to the G_1 cell cycle kinases, such as cyclin D/CDK4 or CDK6 and cyclin E/CDK2, leads to the inhibition of the activities of these kinases (16). To examine the effects of p27 reduction in *Pten*$^{-/-}$ cells on G_1 cell cycle kinase activity, we compared the activities of cyclin E/CDK2 complexes isolated from the synchronized *Pten*$^{+/+}$ and *Pten*$^{-/-}$ cells at various time points after mitotic shake-off. As shown in Fig. 2*C* and quantified in Fig. 2*D*, the loss of PTEN led to an increased level of cyclin E-associated kinase activity, which paralleled the decreased levels of p27 in the *Pten*$^{-/-}$ cells. These studies suggest that the down-regulation of p27 in *Pten*$^{-/-}$ cell may lead to enhanced activation of G_1 cell cycle kinases, which in turn promote advanced S-phase entry.

We also examined the p27 level in asynchronously growing cells. In *Pten*$^{-/-}$ cells, there is a reduction of p27 level by 3- to 4-fold as compared with *Pten*$^{+/+}$ cells (Fig. 2*E*). In contrast, the levels of other G_1 cell cycle regulators, such as cyclin D1, cyclin E, cyclin A, CDK2, as well as cyclin E-associated CDK2 or cyclin A-associated CDK2, did not show significant alteration (Fig. 2*E*). These results suggest that p27 is a selective target for the signaling pathway regulated by the PTEN tumor suppressor.

To address the question of whether the down-regulation of p27 in *Pten*$^{-/-}$ cells occurs at transcriptional or posttranscriptional levels, we compared the 27 mRNA level in *Pten*$^{+/+}$ and *Pten*$^{-/-}$ cells by Northern blot analysis. We found that the level of p27 mRNA was not affected by PTEN status (Fig. 2*F*), suggesting that p27 is modulated by PTEN-regulated signaling pathway at the posttranscriptional level. In addition, the mRNA levels of cyclin D, cyclin E, cyclin A, or CDK2 were not affected by the PTEN status (Fig. 2*F*). Together, these data indicate the loss of PTEN affects cell cycle progression, and one selective target for this process is the down-regulation of p27 at its protein level.

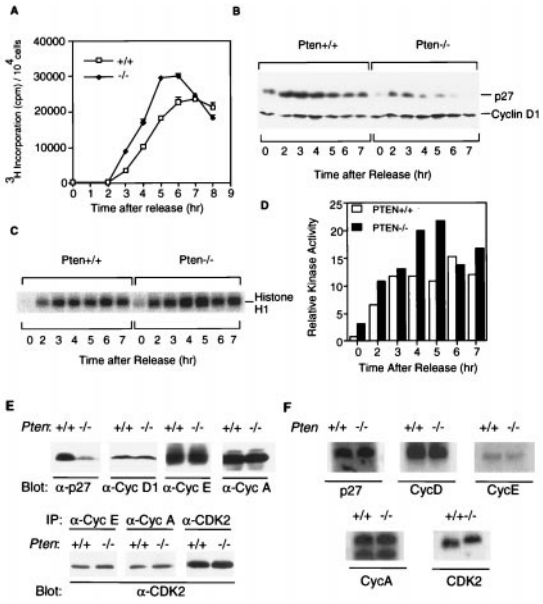

FIG. 2. Cell cycle progression and p27^{KIP1} levels in synchronized and asynchronous *Pten*$^{+/+}$ and *Pten*$^{-/-}$ cells. (*A*) [^{3}H]thymidine incorporation after release from the colcemid block. For each time point, cells (1×10^5) were pulse-labeled with [^{3}H]thymidine (1 μCi/ml) for 1 hr before harvesting. [^{3}H]thymidine incorporation was measured. Each value represents the average (+SD) obtained from duplicate samples. (*B*) Western blot analysis of p27^{KIP1} and cyclin D1 levels after release from colcemid block. Approximately 1×10^6 cells were seeded for each time point, and cell lysates (50 μg each) were examined by Western blot analysis with anti-p27 or anti-cyclin D1 antibody, respectively. (*C* and *D*) Histone H1 kinase activity assay. Cells were synchronized as described in *B*. Cyclin E/CDK2 complex was immunoprecipitated with anti-cyclin E antibody from cell lysates (300 μg each) and assayed for *in vitro* kinase activity by using histone H1 as substrate and ^{32}p-[γ]-ATP. The relative kinase activity was obtained after quantification of the ^{32}P-label incorporated into histone H1 by PhosphorImager. (*E*) Western blot analysis of various cell cycle regulators. Cell lysates from log-phase growing *Pten*$^{+/+}$ or *Pten*$^{-/-}$ cells (50 μg each) were analyzed by Western blot analysis with antibodies specific for p27^{KIP1} or cyclin D1 (*Upper*). To examine the level of cyclin E or cyclin A, cell lysates (2 mg each) were immunoprecipitated with anti-cyclin E or anti-cyclin A antibodies, respectively, followed by Western blot analysis with the corresponding antibodies (*Upper*). (*Lower*) Cell lysates (2 mg each) were immunoprecipitated with antibodies for cyclin E, cyclin A, or CDK2, and analyzed with Western blot analysis with anti-CDK2 antibody. (*F*) Northern blot analysis. Total RNA (5 μg each) harvested from log-phase growing *Pten*$^{+/+}$ or *Pten*$^{-/-}$ cells were subjected to Northern blot analysis using p27, cyclin D, cyclin E, cyclin A, or CDK2 cDNA probe, respectively.

PTEN Down-Regulates PI3 Kinase Signaling by Controlling PIP3 Accumulation. Several signaling pathways are required for cells to progress from G_1 to S phase. Among them, PI3 kinase plays a major role (18). PI3 kinase regulates the production of PIP3, which acts as a second messenger of the PI3 kinase signaling pathway. PTEN can dephosphorylate PIP3 *in vitro* (6), and overexpression of the PTEN gene in human glioblastoma cells results in inhibition of Akt/PKB, a downstream target of PI3 kinase (9). These observations suggest that PTEN potentially may regulate the PI3 kinase signaling pathway.

By using genetically defined *Pten*$^{-/-}$ and *Pten*$^{+/+}$ but otherwise isogenic cells, we examined the levels of PIP3 in cells that have been stimulated with IGF-I. Fig. 3*A* shows a representative result from three independent experiments. *Pten*$^{+/+}$ cells were less sensitive to IGF-I stimulation, and their PIP3 levels were significantly lower than that of *Pten*$^{-/-}$ cells. Five minutes after IGF-I stimulation, only a modest increase in PIP3 level could be detected in *Pten*$^{+/+}$ cells. However, an approximately 2-fold

increase of PIP3 (Fig. 3*B*) over the *Pten*$^{+/+}$ level could be detected in *Pten*$^{-/-}$ ES cells. Even 20 min after stimulation, the PIP3 level in *Pten*$^{-/-}$ ES cells was still very high. In contrast, the levels of PIP and PIP2 were largely unaffected by PTEN deficiency (Fig. 3*A*). The basal level (without IGF-I stimulation) of PIP3 is comparable in *Pten*$^{+/+}$ and *Pten*$^{-/-}$ cells (data not shown). These results suggest that both the magnitude and duration of PIP3 accumulation after IGF-I stimulation were significantly higher in the *Pten*$^{-/-}$ ES cells. This increase in the PIP3 level in *Pten*$^{-/-}$ ES cells is quite reproducible and is comparable to the elevated PIP3 level induced by the overexpression of a constitutive active form of PI3 kinase (form p110*), as reported (19). These findings suggest that PIP3 is an intracellular target of PTEN.

Increased Phosphorylation and Activation of PKB/Akt in *Pten*$^{-/-}$ ES Cells Correlates with Cell Proliferation and Down-Regulation of p27^{KIP1}. PKB/Akt, a growth factor-regulated serine/threonine kinase, is one of the best-characterized downstream targets of PIP3. Akt is activated by its association with PIP3, which facilitates Akt phosphorylation and activation by the upstream kinases (PDK1 and PDK2) (20). We examined Akt phosphorylation in *Pten*$^{+/+}$ and *Pten*$^{-/-}$ cells after IGF-I stimulation. In *Pten*$^{+/+}$ ES cells, IGF-I induced a transient but modest phosphorylation of Akt on serine-473, which can be detected by a specific diagnostic antibody (Fig. 4*A*, *Left*). Akt phosphorylation reached its highest level around 20–40 min and subsequently was down-regulated by 90 min. In *Pten*$^{-/-}$ ES cells, both the basal level and the magnitude of Akt phosphorylation were significantly increased (Fig. 4*A*, *Right*). The duration of Akt phosphorylation also was prolonged, as no significant down-regulation of Akt phosphorylation could be observed in *Pten*$^{-/-}$ cells even 90 min after IGF-I stimulation. The sustained high level of Akt phosphorylation in *Pten*$^{-/-}$ cells suggests that the increase in PIP3 accumulation caused by PTEN deficiency is sufficient to induce the activation of Akt.

Because the selective growth advantage of *Pten*$^{-/-}$ ES cells was observed under normal culture conditions, we also examined whether the steady state of phosphorylated Akt is affected by the PTEN deficiency. As shown in Fig. 4*B*, we found that the level of Akt phosphorylation was very sensitive to the dosage of the *Pten* gene. The phosphorylated form of Akt could be detected in *Pten*$^{+/+}$ cells. In *Pten*$^{+/-}$ cells, a noticeable increase in Akt phosphorylation was observed. In *Pten*$^{-/-}$ cells, this increase became even more dramatic (Fig. 4*B*). Such changes of Akt status occurred only at the level of phosphorylation and therefore its activation; no changes in the protein level of Akt could be detected in these assays (Fig. 4*B*). We further examined whether Akt phosphorylation correlated with the growth status of the cells. As shown in Fig. 4*C*, in the lysates prepared from actively growing cells, there was a significant increase of Akt phosphorylation in two independent *Pten*$^{-/-}$ ES clones as compared with *Pten*$^{+/+}$ cells. This increase became less obvious when cells were harvested upon reaching confluence (Fig. 4*C*). In parallel, we also examined the level of p27^{KIP1}. Similar to changes of phosphorylation of Akt, the difference of the p27 levels in *Pten*$^{+/+}$ and *Pten*$^{-/-}$ cells was most pronounced in log-phase growing cells (Fig. 4*C*). As a control, the levels of cyclin D1 were independent of the PTEN status and the growth state of the cell (Fig. 4*C*). These observations raise the possibility that Akt, or other molecules activated by PIP3, may be involved in down-regulation of p27^{KIP1} and promoting cell proliferation.

To examine whether the increased PIP3 accumulation and Akt activation in *Pten*$^{-/-}$ cells is caused by up-regulation of PI3 kinase, we analyzed the tyrosine phosphorylation status of PI3 kinase itself in *Pten*$^{-/-}$, *Pten*$^{+/-}$, and *Pten*$^{+/+}$ cells. The PI3 kinase, the p85/p110 heterodimer, is activated by tyrosine phosphorylation on the p85 regulatory subunit (18). No significant alteration on p85 tyrosine phosphorylation could be detected in *Pten*$^{-/-}$ cells (Fig. 4*D*). These results suggest that PTEN functions downstream of PI3 kinase and that the elevated PIP3 level in *Pten*$^{-/-}$ ES cells is likely caused by impaired dephosphorylation of PIP3 by loss of PTEN rather than increased production by PI3 kinase.

To determine whether PTEN deficiency affects signaling molecules other than Akt, we examined phosphorylation status of MAPK and FAK. Our experiment revealed that the tyrosine phosphorylation and thus the activated forms of MAPK were not affected by the *Pten* deletion (Fig. 4*D*). It was reported that FAK could interact with and be dephosphorylated by PTEN in cells overexpressing PTEN (21). However, no significant difference in FAK phosphorylation could be detected among *Pten*$^{-/-}$, *Pten*$^{+/-}$, and *Pten*$^{+/+}$ cells (Fig. 4*D*). Thus, our studies suggest that PTEN selectively regulate the PIP3/Akt signaling pathway.

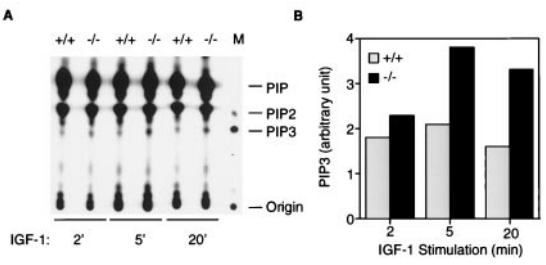

FIG. 3. PIP3 accumulation in *Pten*$^{+/+}$ and *Pten*$^{-/-}$ cells. (*A*) PIP3 levels in *Pten*$^{+/+}$ and *Pten*$^{-/-}$ ES cells after IGF-I stimulation. Cells were starved in a serum-free medium for 16 hr, and then labeled with [^{32}P]orthophosphate (0.5 mCi/ml) for 2 hr. Cells then were stimulated by IGF-I (1 μg/ml) for 2, 5, or 20 min before harvesting. Phospholipids were extracted and analyzed on a TLC plate. Assignment of PIP, PIP2, and PIP3 was done according to *in vitro* ^{32}P-labeled phosphoinositides standards (see *Materials and Methods*). In lane M, [^{32}P]-labeled PIP3 is shown as a marker. (*B*) Quantitation of PIP3 levels in *Pten*$^{+/+}$ and *Pten*$^{-/-}$ ES cells after IGF-I stimulation. The amount of radioactivity corresponding to PIP3 was measured with a PhosphorImager and presented as an arbitrary unit.

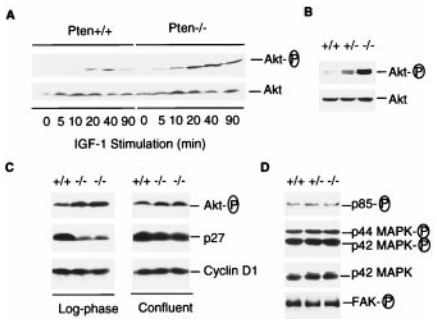

FIG. 4. Phosphorylation status of Akt, PI3 kinase, MAPK, and FAK, and the levels of p27 in *Pten*$^{+/+}$, *Pten*$^{+/-}$, or *Pten*$^{-/-}$ ES cells. (*A*) Phosphorylation status of Akt after IGF-I stimulation. *Pten*$^{+/+}$ and *Pten*$^{-/-}$ ES cells were passed twice without feeders to reduced background. Cells were serum-starved for 34 hr, then stimulated by IGF-I (1 μg/ml) for indicated time periods. Cell lysates (25 μg each) were examined by Western blot analysis with antibodies against phospho-Akt (serine-473) or Akt, respectively. (*B*) Phosphorylation status of Akt in actively growing ES cells. Log-phase growing *Pten*$^{+/+}$, *Pten*$^{+/-}$, or *Pten*$^{-/-}$ ES cells were harvested, and the cell lysates were analyzed with antibodies against phospho-Akt or Akt, respectively. (*C*) Akt, p27^{KIP1}, and cyclin D1 levels in cells from different proliferation states. Cells were harvested from either log-phase cultures (*Left*) or confluent cultures (*Right*). Cell lysates (50 μg each) were examined by Western blot analysis with antibody specific for phospho-Akt, p27, or cyclin D1, respectively. (*D*) Phosphorylation status of PI3 kinase, MAPK, and FAK. Cell lysates were prepared from log-phase growing cells. To determine the phosphorylation status of the p85 subunit of PI3 kinase and FAK, cell lysates (500 μg each) were immunoprecipitated with antiphosphotyrosine antibody 4G10 followed by Western blot analysis with anti-p85 or anti-FAK antibody, respectively. To detect phosphorylated p42 and p44 MAPK, cell lysates (50 μg each) were examined by Western blots analysis with an antibody against phospho-MAPK. As a control, a duplicate filter was analyzed in parallel with an antibody for p42 MAPK.

An Increased Akt Activation in *Pten*$^{-/-}$ MEF Cells Leads to Increased Phosphorylation of Bad and Cell Survival. ES cells are stem cells and represent the most undifferentiated cell type with high proliferative potential. Because of the unique status of ES cells, we were interested in determining whether inactivation of PTEN produced similar effects (e.g., increased growth rate and activation of Akt) in more differentiated cell types such as MEF cells. To generate *Pten*$^{-/-}$ MEF cells, we injected several lines of *Pten*$^{-/-}$ ES cells into blastocysts, and *Pten*$^{-/-}$ MEF were obtained from embryonic day 14–15 chimeric embryos after G418 selection to eliminate WT MEF cells. Complete inactivation of PTEN was confirmed by both Southern (data not shown) and Western blot analyses (Fig. 5*A*). During the course of culturing *Pten*$^{+/+}$ and *Pten*$^{-/-}$ MEF cells, we did not observe significant differences in the rate of growth, nor at the level of p27^{KIP1} (data not shown), possibly because of the differences in the cell cycle checkpoint control mechanism between ES and MEF cells (see *Discussion*).

Similar to *Pten*$^{-/-}$ ES cells, *Pten*$^{-/-}$ MEF cells contained a modest increase in PIP3 level (data not shown) and a significant enhancement in phosphorylation of Akt, as compared with their *Pten*$^{+/+}$ counterparts. Again, the total protein level of Akt was not affected (Fig. 5*A*). In addition, no detectable changes were observed for the level and phosphorylation status of MAPK (data not shown).

To demonstrate the causal relationship between the loss of PTEN and activation of Akt, we reintroduced either the WT *PTEN* gene or its mutant derivative *PTEN* CS back into *Pten*$^{-/-}$ cells by the retrovirus-mediated expression system. The *PTEN* CS mutant contains a substitution of the cysteine 124 with serine at the phosphatase signature motif and is catalytically inactive (3). Although Akt phosphorylation in *Pten*$^{-/-}$ MEF cells was significantly decreased upon reintroduction of the WT *PTEN* gene, no difference could be detected when *PTEN* CS was overexpressed (Fig. 5*A*, *Right*). These data reinforce the idea that Akt phosphorylation level depends on the *PTEN* gene dosage and that the phosphatase activity of PTEN is required for Akt inactivation.

Activation of Akt is essential for cell survival after growth factor withdrawal (20). To determine whether the increased Akt activity by PTEN deletion is sufficient to trigger downstream events, especially the growth survival effect of Akt, we examined the phosphorylation status of Bad, a member of the Bcl2 family. Bad can be phosphorylated by Akt, and such phosphorylation causes the loss of pro-apoptotic activity of Bad (22, 23). As shown in Fig. 5*B*, *Pten*$^{-/-}$ cells contained higher levels of phosphorylated Bad as compared with its *Pten*$^{+/+}$ counterparts, either in the presence or the absence of IGF-I stimulation. These data suggest that the Akt-controlled anti-cell death pathway is up-regulated and activated in *Pten*$^{-/-}$ cells.

To examine whether the increased phosphorylation of Akt and Bad affects MEF cell survival, we subjected *Pten*$^{+/+}$ and *Pten*$^{-/-}$ MEF cells to serum withdrawal. At different time points during serum starvation, cells were harvested and analyzed by two different procedures. First, we stained cells with propidium iodide and determined cell viability by fluorescence-activated cell sorting analysis. As summarized in Fig. 5*C*, the WT and *Pten*$^{-/-}$ MEF cells had significantly different survival rates in response to serum starvation. After serum starvation for 4 days, death occurred in more than 60% of WT cells, whereas fewer than 30% of *Pten*$^{-/-}$ cells underwent apoptosis. Second, TUNEL assays were performed to detect apoptotic cells by *in situ* staining. No significant cell death occurred in either population when cells were cultured under optimal growth conditions (Fig. 5*D*, *a* and *b*). However, 72 hr after serum withdrawal, a high incidence of apoptosis was observed in *Pten*$^{+/+}$ but not in *Pten*$^{-/-}$ MEF cultures (Fig. 5*D*, *c* and *d*). These data suggest that inactivation of PTEN leads to up-regulation of the AKT pathway and prevents cells from apoptotic death.

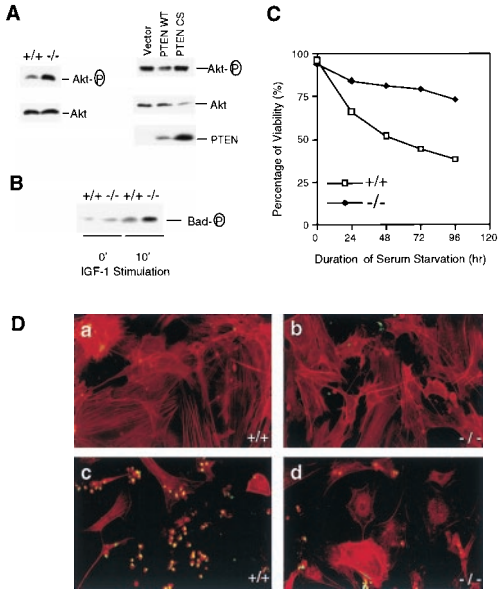

FIG. 5. Increased phosphorylation of Akt and Bad promotes *Pten*$^{-/-}$ MEF cells survival. (*A*, *Left*) MEF cell lysates were prepared and subjected to Western blot analyses as described in the legend of Fig. 4*B*. (*A*, *Right*) *Pten*$^{-/-}$ MEF cells were infected with retroviruses carrying empty vector, the WT PTEN, or the PTEN CS mutant. Cells were harvested 48 hr postinfection. Cell lysates (50 μg each) were subjected to Western blot analysis with antibodies specific for phospho-Akt or Akt, respectively. A duplicate filter also was analyzed with anti-PTEN antibody. (*B*) MEF cells were serum-starved for 16 hr, then labeled with [^{32}P]orthrophosphate for 4 hr. Cells then were stimulated with IGF-I (1 μg/ml) for 10 min before harvest. Cell lysates were subjected to immunoprecipitation with anti-Bad antibody, and the immunoprecipitates were analyzed by SDS/PAGE and autoradiography. (*C*) Propidium iodide staining. *Pten*$^{+/+}$ or *Pten*$^{-/-}$ MEF cells were seeded in serum-free medium. At the indicated time, cells (both adherent and in suspension) were collected and stained with isotonic propidium iodide solution. Percentage of cell viability, determined by using fluorescence-activated cell sorting analysis, is presented. (*D*) TUNEL assay. Log-phase *Pten*$^{+/+}$ (*a* and *c*) and *Pten*$^{-/-}$ (*b* and *d*) MEF cells were grown with (*a* and *b*) or without (*c* and *d*) serum for 72 hr. Cells were stained with TUNEL reaction mix (green) and counterstained with rhodamine-phalloidin (red). Apoptotic cells were indicated by positive staining with both TUNEL reaction mix and pholloidin dye (yellow).

DISCUSSION

By using a genetically defined system, we have demonstrated that PTEN negatively regulates PIP3 and Akt signaling pathway. Several lines of evidence suggest that accumulation of PIP3 in *Pten*$^{-/-}$ cells is caused by the loss of PTEN phosphatase activity. First, we have shown that the activity of PI3 kinase, the enzyme that specifically produces PIP3, was not altered in *Pten*$^{-/-}$ ES cells. Thus the observed higher PIP3 levels in *Pten*$^{-/-}$ cells is likely caused by the decreased dephosphorylation of PIP3. Second, we showed that by reintroducing the WT *PTEN* gene into *Pten*$^{-/-}$ MEF cells, we could reverse PIP3-dependent Akt activation. Such a reversion requires the phosphatase activity of PTEN, suggesting that PTEN is likely to be a bona fide phosphatase for PIP3. Our data are further supported by the results from previous experiments, which showed that PTEN could act as a specific phosphoinositide 3-phosphatase *in vitro* and overexpression of PTEN in 293 cells resulted in decreased PIP3 levels (6).

We have further demonstrated that Akt/PKB, a downstream target for PIP3 signaling, is up-regulated in PTEN-deficient cells. Akt phosphorylation and activation depend on the dosage as well as the phosphatase activity of the Pten gene product. In log-phase growing *Pten*$^{-/-}$ cells, the steady-state level of Akt phosphorylation is 3- to 4-fold higher than *Pten*$^{+/+}$ cells. Moreover, Akt activation directly correlates with the proliferation state of the cells. A direct role of Akt in cell cycle progression has been

suggested by the recent observation that expression of a constitutive activated Akt in mouse macrophage cells or rat fibroblasts can trigger S-phase entry in the absence of serum growth factors (24, 25). Together, these results indicate that Akt may be a critical molecule involved in the regulation of normal cell growth.

$p27^{KIP1}$ has been proposed to prevent unscheduled activation of cyclin-CDK complexes in G_1 phase (16). Several reports (9, 26–28) suggest that PI3 kinase signaling may be involved in the down-regulation of p27. In NIH 3T3 cells, expression of a dominant-negative form of Ras, probably through inhibition of PI3 kinase, can block cell cycle progression at mid or late G_1 phase (26, 27). In aortic smooth muscle cells, treatment of cells with wortmannin, a pharmacologic inhibitor for PI3 kinase, also blocked G_1 cell cycle progression (28). In both systems, the G_1 cell cycle block was accompanied by failure to down-regulate p27 (26–28). We recently observed that in U87MG human glioblastoma cells transient expression of PTEN leads to significant up-regulation of p27 and G_1 cell cycle arrest (9). However, it is unclear from these experiments whether the increased $p27^{KIP1}$ level is the cause or the consequence of G_1 cell cycle arrest.

In this study, we have provided *in vivo* evidence that $p27^{KIP1}$ is a downstream target of the PIP3 signaling pathway and such regulation occurs at the posttranscriptional level. Our studies suggest that down-regulation of $p27^{KIP1}$ is likely to be a critical or even a rate-limiting step during G_1/S transition in ES cells. We have attempted to reintroduce the *PTEN* gene into $PTEN^{-/-}$ ES cells to rescue the cell-cycle regulation defect. However, we failed to obtain stable cell clones that expressed the exogenous *PTEN* gene (data not shown). This failure was likely caused by the growth suppression effect of overexpressed PTEN in these cells, a phenomenon similar to that observed in human glioblastoma cells (7–9). It is interesting to point out that down-regulation of $p27^{KIP1}$ and advanced cell cycle progression are most notable in $Pten^{-/-}$ ES cells, but are less obvious in more differentiated MEF cells. Such differential cell responses may reflect the differences in intrinsic cell cycle control mechanisms between these two cell types. Down-regulation of $p27^{KIP1}$ by PIP3 signaling may be sufficient for cell cycle progression in ES cells, whereas in MEF cells additional signaling processes may be required. This scenario is consistent with tumorigenesis in animals and humans. Mice lacking $p27^{KIP1}$ suffer from multiple organ hyperplasia (29–31). A common feature among these organs is that their progenitor cells are undifferentiated and mitotically active. Many tumor cells also arise from undifferentiated progenitor cells, and the mutation in the PTEN gene in those cells may be sufficient to promote cell cycle progression. It is interesting to note that PTEN mutations frequently are observed in advanced human prostate cancer (32) and the levels of p27 inversely correlate with prognosis of prostate cancer (33). It is possible that the decreased $p27^{KIP1}$ level in prostate cancer tissues occurs as a consequence of impaired PTEN function.

While this manuscript was under review, Stambolic *et al.* (34) reported that immortalized $Pten^{3-5}$ (disruption of exons 3–5 of the murine *Pten* gene) MEF cells exhibited resistance to cell death stimuli, accompanied by increases of PIP3 level and Akt activation. Their conclusion that PTEN regulates apoptosis is consistent with part of the conclusion discussed in this paper. They also observed that a prominent feature in $Pten^{-/-}$ embryos was enhanced cell proliferation during early embryogenesis, although they had not provided a mechanistic explanation for this phenotype. Di Cristofano (10) *et al.* recently reported that PTEN is essential for embryonic development, and $Pten^{+/-}$ mice or chimaeric mice derived from $Pten^{+/-}$ ES cells show hyperplastic-dysplastic changes in prostate, skin, and colon, and the mice also develop germ cell, gonadostroma, thyroid, and colon tumors. These observations further highlight the importance of PTEN in regulation of cell proliferation, and our findings of PTEN deficiency having a profound effect on cell cycle progression provides a molecular basis for these phenotypes.

In summary, our studies reveal an insight into the mechanism by which PTEN functions as a tumor suppressor. By regulating PIP3 and Akt/PKB, PTEN modulates two fundamental cellular processes: cell cycle progression and cell survival. Alteration of either or both processes has long been implicated in the genesis of human cancer.

We thank Drs. Harvey Herschman, Sam Chow, Des Smith, and Owen Witte and members of our laboratories for critical reading of the manuscript. We thank Drs. Alexis Traynor-Kaplan and Andrew Morris for advice on the phospholipid analysis. R.L. was a Howard Hughes Postdoctoral Associate and currently is supported by the Deutsche Forschungsgemeinschaft and CapCure fund. D-M.L. was a recipient of the Leslie H. Warner Fellowship in Cancer Research. H.S. is a Pew Scholar in the Biomedical Sciences. H.W. is an Assistant Investigator of the Howard Hughes Medical Institute and V Foundation Scholar. This work was supported by grants from the Pew Charitable Trust and the Department of the Army (DAMD 17-98-1-8271) (H.S.), National Institutes of Health (CA72878) (H.Z.), and the V Foundation and CapCure Fund (H.W.).

1. Li, J., Yen, C., Liaw, D., Podsypanina, K., Bose, S., Wang, S. I., Puc, J., Miliaresis, C., Rodgers, L., McCombie, R., *et al*. (1997) *Science* **275,** 1943–1947.
2. Steck, P. A., Pershouse, M. A., Jasser, S. A., Lin, H., Yung, W. K. A., Ligon, A. H., Langford, L. A., Baumgard, M. L., Hattier, T., Davis, T., *et al*. (1997) *Nat. Genet.* **15,** 356–363.
3. Li, D.-M. & Sun, H. (1997) *Cancer Res.* **57,** 2124–2129.
4. Eng, C. (1998) *Int. J. Oncol.* **12,** 701–710.
5. Myers, M. P., Stolarov, J. P., Eng, C., Li, J., Wang, S. I., Wigler, M. H., Parsons, R. & Tonks, N. K. (1997) *Proc. Natl. Acad. Sci. USA* **94,** 9052–9057.
6. Maehama, T. & Dixon, J. E. (1998) *J. Biol. Chem.* **273,** 13375–13378.
7. Furnari, F. B., Lin, H., Huang, H. J. S. & Cavenee, W. K. (1997) *Proc. Natl. Acad. Sci. USA* **94,** 12479–12484.
8. Cheney, I. W., Johnson, D. E., Vaillancourt, M. T., Avanzini, J., Morimoto, A., Demers, G. W., Wills, K. N., Shabram, P. W., Bolen, J. B., Tavtigian, S. V. & Bookstein, R. (1998) *Cancer Res.* **58,** 2331–2334.
9. Li, D.-M. & Sun, H. (1998) *Proc. Natl. Acad. Sci. USA* **95,** 15406–15411.
10. Di Cristofano, A., Pesce, B., Cordon-Cardo, C. & Pandolfi, P. P. (1998) *Nat. Genet.* **19,** 348–355.
11. Wu, H., Liu, X. & Jaenisch, R. (1994) *Proc. Natl. Acad. Sci. USA* **91,** 2819–2823.
12. Savatier, P., Huang, S., Szekely, L., Wiman, K. G. & Samarut, J. (1994) *Oncogene* **9,** 809–818.
13. Zhang, H., Kobayashi, R., Galaktionov, K. & Beach, D. (1995) *Cell* **82,** 915–925.
14. Traynor-Kaplan, A. E., Thompson, B. L., Harris, A. L., Taylor, P., Omann, G. M. & Sklar, L. A. (1989) *J. Biol. Chem.* **264,** 15668–15673.
15. Serunian, L. A., Auger, K. R. & Cantley, L. C. (1991) *Methods Enzymol.* **198,** 78–87.
16. Hunter, T. & Pines, J. (1994) *Cell* **79,** 573–582.
17. Aladjem, M. I., Spike, B. T., Rodewald, L. W., Hope, T. J., Klemm, M., Jaenisch, R. & Wahl, G. M. (1998) *Curr. Biol.* **8,** 145–155.
18. Toker, A. & Cantley, L. C. (1997) *Nature (London)* **387,** 673–676.
19. Klippel, A., Reinhard, C., Kavanaugh, W. M., Apell, G., Escobedo, M. A. & Williams, L. T. (1996) *Mol. Cell. Biol.* **16,** 4117–4127.
20. Downward, J. (1998) *Curr. Opin. Cell. Biol.* **10,** 262–267.
21. Tamura, M., Gu, J., Matsumoto, K., Aota, S., Parsons, R. & Yamada, K. M. (1998) *Science* **280,** 1614–1617.
22. Datta, S. R., Dudek, H., Tao, X., Masters, S., Fu, H., Gotoh, Y. & Greenberg, M. E. (1997) *Cell* **91,** 231–241.
23. del Peso, L., Gonzalez-Garcia, M., Page, C., Herrera, R. & Nunez, G. (1997) *Science* **278,** 687–689.
24. Ahmed, N. N., Grimes, H. L., Bellacosa, A., Chan, T. O. & Tsichlis, P. N. (1997) *Proc. Natl. Acad. Sci. USA* **94,** 3627–3632.
25. Klippel, A., Escobedo, M. A., Wachowicz, M. S., Apell, G., Brown, T. W., Giedlin, M. A., Kavanaugh, W. M. & Williams, L. T. (1998) *Mol. Cell. Biol.* **18,** 5699–5711.
26. Takuwa, N. & Takuwa, Y. (1997) *Mol. Cell. Biol.* **17,** 5348–5358.
27. Aktas, H., Cai, H. & Cooper, G. M. (1997) *Mol. Cell. Biol.* **17,** 3850–3857.
28. Bacqueville, D., Casagrande, F., Perret, B., Chap, H., Darbon, J. M. & Breton-Douillon, M. (1998) *Biochem. Biophys. Res. Commun.* **244,** 630–636.
29. Fero, M. L., Rivkin, M., Tasch, M., Porter, P., Carow, C. E., Firpo, E., Polyak, K., Tsai, L. H., Broudy, V., Perlmutter, R. M., *et al*. (1996) *Cell* **85,** 733–744.
30. Kiyokawa, H., Kineman, R. D., Manova-Todorova, K. O., Soares, V. C., Hoffman, E. S., Ono, M., Khanam, D., Hayday, A. C., Frohman, L. A. & Koff, A. (1996) *Cell* **85,** 721–732.
31. Nakayama, K., Ishida, N., Shirane, M., Inomata, A., Inoue, T., Shishido, N., Horii, I., Loh, D. Y. & Nakayama, K. (1996) *Cell* **85,** 707–720.
32. Cairns, P., Okami, K., Halachmi, S., Halachmi, N., Esteller, M., Herman, J. G., Isaacs, W. B., Bova, G. S. & Sidransky, D. (1997) *Cancer Res.* **57,** 4997–5000.
33. Cordon-Cardo, C., Koff, A., Drobnjak, M., Capodieci, P., Osman, I., Millard, S. S., Gaudin, P. B., Fazzari, M., Zhang, Z. F., Massague, J. & Scher, H. I. (1998) *J. Natl. Cancer Inst.* **90,** 1284–1291.
34. Stambolic, V., Suzuki, A., de la Pompa, J. L., Brothers, G. M., Mirtsos, C., Sasaki, T., Ruland, J., Penninger, J. M., Siderovski, D. P. & Mak, T. W. (1998) *Cell* **95,** 29–39.